

# Where does all the phosphorus go? Mass balance modelling of phosphorus in the Swedish long-term soil fertility experiments

Jon Petter Gustafsson<sup>a,\*</sup>, Florian Barbi<sup>a,b</sup>, Sabina Braun<sup>a</sup>, Wantana Klysubun<sup>c</sup>, Gunnar Börjesson<sup>a</sup>

<sup>a</sup> Department of Soil and Environment, Swedish University of Agricultural Sciences, SE-750 07 Uppsala, Sweden

<sup>b</sup> Current Address: Institute of Microbiology of the Czech Academy of Sciences, Vídeňská 1083, 14220 Praha 4, Czech Republic

<sup>c</sup> Synchrotron Light Research Institute, 111 Moo 6 University Avenue, Muang District, 30000 Nakhon Ratchasima, Thailand

## ARTICLE INFO

Handling Editor: D. Said-Pullicino

### Keywords:

Mass balance model  
Speciation  
XANES  
Diffusion  
Adsorption  
Leaching

## ABSTRACT

To gain insights into phosphorus (P) dynamics in soils and the ability to predict soil responses to varying fertilizer inputs, mass balance models prove to be valuable tools. In this study, a new dynamic mass balance model, PBalD8, was used to describe the change in extracted P in the A horizon of soils subjected to diverse fertilizer treatments over a period of 50 to 60 years in five soil fertility experiments. The model employed a Freundlich equation to describe soil-solution partitioning of P and assumed that acid-lactate-extractable P represented a labile pool of P in instant equilibrium with soil solution P. Additionally, oxalate-extractable inorganic P was presumed to comprise the sum of the labile and stable pools of P, with mass flux to and from the latter described by Fick's first law. The model was evaluated using results from extractions and P K-edge XANES spectroscopy. Notably, organic P, as revealed by P K-edge XANES, did not substantially contribute to long-term changes in soil P content and was therefore excluded from consideration. In general, the model offered reasonable fits to the extracted P concentrations. However, for the P-depleted treatments, a prerequisite was that the P removal through harvest was lower compared to measurements. Conversely, in three of the soils, the modelled fertilizer inputs needed to be reduced to 70 % to 85 % of the known additions. These discrepancies may be attributed to the involvement of deeper soil horizons, including deep crop uptake and mixing with lower soil layers, although other factors such as lateral dispersion and inaccuracies in estimating applied fertilizers cannot be discounted. These results underscore the necessity of gaining a more comprehensive understanding of how deeper soil horizons influence P mass balances in agricultural soils. In one of the soils, Fjärdingslöv, P K-edge XANES results demonstrated the formation of calcium phosphate over time in the highest fertilization treatment, consistent with the model. Additionally, in two soils, Kungsängen and the P-depleted Vreta Kloster soil, the model predicted a significant contribution from mineral weathering. However, the PBalD8 model also projected higher P leaching rates than those observed, suggesting that the model may not fully capture this P output term.

## 1. Introduction

Optimum P (phosphorus) fertilization is key to successful nutrient management. Excessive P loads may lead to P leaching, which may cause eutrophication in surface waters (Römkens and Nelson, 1974). Low fertilizer inputs may lead to suboptimal crop growth and thus to low harvest yields (Jordan-Meille et al., 2012). A common strategy for optimum P fertilization is to find the amount of fertilizer input of P that is exactly balanced by the offtake of P through harvest (Bertilsson et al., 2005; Jordan-Meille et al., 2012). However, a requirement for this

simple approach to work is that the soil is close to steady state with respect to a given total input of P. Long-term fertility experiments, where different fertilizer application rates have been maintained for decades, serve as invaluable sources of data for establishing optimal P input levels within a balanced fertilization strategy. Several studies utilizing such datasets have established P balances by closely monitoring the P quantities removed in harvested crops and comparing them to fertilizer inputs, net changes in soil P pools, and atmospheric deposition (Jaakkola et al., 1997; Messiga et al., 2012; Morel et al., 2014; González Rodríguez et al., 2018; Azeez et al., 2020). However, these assessments

\* Corresponding author.

E-mail address: [jon-petter.gustafsson@slu.se](mailto:jon-petter.gustafsson@slu.se) (J.P. Gustafsson).

<https://doi.org/10.1016/j.geoderma.2023.116727>

Received 24 May 2023; Received in revised form 20 November 2023; Accepted 27 November 2023

Available online 3 December 2023

0016-7061/© 2023 The Author(s). Published by Elsevier B.V. This is an open access article under the CC BY license (<http://creativecommons.org/licenses/by/4.0/>).

are often complicated by several factors, including: (i) the challenge of accurately estimating P leaching from the soil volume (Azeez et al., 2020); (ii) the exchange of P between the topsoil and deeper soil horizons, potentially driven by mechanisms such as deep root uptake and bioturbation, which are challenging to quantify (De Bolle et al., 2013; Siebers et al., 2021); (iii) potential lateral spread of applied fertilizers to neighboring plots (Sibbesen et al., 2000).

A process that delays the soil response to changes in P input and is key to P mass-balance modeling is the adsorption/desorption of P (i.e.,  $\text{PO}_4\text{-P}$ ) to Fe(III) and Al(III) (hydr)oxides. This process involves the formation of surface complexes on singly coordinated oxygens on the (hydr)oxide surface and is expected to become increasingly important at low pH (e.g. Goldberg and Sposito, 1984; Hiemstra and van Riemsdijk, 1996). We have earlier found adsorption/desorption of P to be the most important process that stores or releases P in response to a change in fertilizer input over time scales of years to decades, while the stores of organic P show much less, if any, change (Eriksson et al., 2016; Braun et al., 2019). Precipitation/dissolution of Ca phosphates may also contribute to the response in soil P, but to a lower extent, except in calcareous soils (Braun et al., 2019). Varying amounts of organic P, e.g. as inositol phosphates, may also be adsorbed (Celi et al., 1999). The exact role of organic P is unknown, however, partly because of the difficulty of distinguishing between adsorbed inorganic and organic P with P K-edge XANES spectroscopy (Gustafsson et al., 2020). In the following, we treat P adsorption/desorption as a process that primarily involves inorganic P, but we do not exclude the possibility that the adsorbed P pool consists of a contribution of organic P, which in some cases may be substantial.

In itself, P adsorption/desorption may be slow over long time periods due to slow diffusion rates to and from the porous Fe and Al (hydr)oxide solids where P is adsorbed (Barrow and Shaw, 1975; McGechan and Lewis, 2002). Often in the soil science literature, a distinction is made between two pools, i.e., a “fast” or “labile” pool of adsorbed P that reacts quickly with the soil solution (in the order of hours to days), and a “slow” or “stable” pool that equilibrates only very slowly. Commonly, the quantity of P obtained from common soil tests such as acid ammonium lactate (AL) (Egnér et al., 1960) or sodium bicarbonate buffer (“Olsen”) (Olsen et al., 1954) is assumed to represent a “fast” or plant-available P pool that crops can access within a reasonably short time frame. However, the extent to which these extractions can quantify this P pool remains a matter of debate (Mundus et al., 2017; Braun et al., 2019).

Many efforts have been made to derive relationships for the slow diffusion of P into or out from the “slow” or “stable” P pool (Lookman et al., 1995; McGechan and Lewis, 2002). In some approaches, Fick’s first law, according to which the diffusive flux of P results from simple mass transfer and is proportional to the concentration difference between the solid and bulk solution phases, was used (Koopmans et al., 2004; Smolders et al., 2021). A related approach was taken by Jones et al. (1984) in their EPIC model, except that three different inorganic P pools were distinguished, i.e., the labile, active, and stable P, and that the fluxes between them were defined relative to the solid-phase concentrations of P. This is consistent with Fick’s first law if the dissolved P concentration in the porous solid is linearly related to the sorbed concentration (i.e., linear isotherm). The EPIC model equations were later integrated into the CREAMS/GLEAMS/ICECREAM family of models, with some modifications (Sharples et al., 1984; Tattari et al., 2001). A large number of other more sophisticated approaches have been suggested. For example, one may assume that diffusion is driven to a large extent by chemical and electrostatic interactions between the charged (hydr)oxide surfaces in the porous solid and dissolved P (Barrow, 1983). In the unreacted shrinking core (USC) model, it is assumed that P does not penetrate the oxide but instead gradually converts the oxide to a metal phosphate, the rate of which depends on the diffusion of P into the oxide core (van der Zee and van Riemsdijk, 1988). Freese et al. (1995) reformulated the latter model by removing a term and by combining it

with a Langmuir equation to describe P sorption kinetics in a more general sense.

Several difficulties are encountered when testing and evaluating dynamic P mass-balance models for a real field situation, such as long-term soil fertility experiments in which different amounts of fertilizer were added. First, for “calibration,” the modeller usually has to rely on extractions carried out within the experimental programme to quantify the different P pools, such as acid ammonium lactate (AL) and Olsen extractions to quantify “fast” or labile P, and oxalate-extractable P or pseudo-total P to quantify the total amount of geochemically active P. Second, there may be cross-contamination between adjacent plots due to tillage, soil erosion, etc. (Sibbesen et al., 2000). Third, the experimental programme often only includes samples from the A horizon, making it difficult to address the effects of deep root uptake and bioturbation (see, e.g., Rubaek et al., 2013; Siebers et al., 2021). Fourth, to properly initialize the model, there is a need for data on fertilization and P offtake for several hundred years prior to the start of the soil fertility experiments. As such data typically do not exist, crude assumptions are needed, which create additional uncertainty (van der Salm et al., 2016). For these reasons, simple models (such as, for example, those built around Fick’s first law of diffusion), which are easy to set up and calibrate, may actually prove to be more useful than the more sophisticated model approaches.

In this paper, we test an approach to describe the development of acid ammonium lactate (AL) and oxalate-P over several decades in five Swedish non-calcareous soils subject to different fertilization regimes. This is realized using a new mass balance model, PBalD8, which is based on Fick’s first law and, when properly calibrated, could be able to predict long-term fertilizer requirements. The results are compared also to the solid-phase speciation of P as obtained by P K-edge XANES (X-ray absorption near-edge structure) spectroscopy.

## 2. Materials and methods

### 2.1. Experimental sites and soil sampling

Soil samples were taken from five of the Swedish soil fertility experiments: Ekebo, Fjärdingslöv, Högåsa, Kungsängen, and Vreta Kloster (see Table 1 for geographical locations and general soil properties). The experiments had a split-plot experimental design consisting of two crop rotations, one for a farm with dairy production and one for a farm without livestock (Kirchmann, 1991; Kirchmann et al., 1999; Carlgren and Mattsson, 2001; Kirchmann et al., 2005). Only the latter rotation was utilized in the current study; specifically, mineral fertilizer, rather than manure, was employed to generate plots with varying P status. In the treatments studied, four levels of P and potassium (K) addition were used while the N fertilizer input was the same in all plots (Table 1). Fertilizer N was added as Nitro Chalk (28 % N), fertilizer K was added as potassium chloride (50 % K), and fertilizer P was added as single superphosphate (9 % P) until 1991 (Ekebo and Fjärdingslöv) or 1994 (other sites) and as triple superphosphate (20 % P) thereafter. There were two replicates of each treatment. Throughout the experimental period, ten subsamples from the center of both replicates of each plot were collected with a soil corer ( $\varnothing = 2$  cm) to a depth of 20 cm. The subsamples were then combined and homogenized. The soil samples were air-dried at room temperature for 7 days, crushed with a wooden pestle, and passed through a 2 mm sieve.

### 2.2. General soil properties, extractable P fractions, and P sorption experiments

For samples collected in 2017, the particle-size distribution was determined using the pipette method (ISO, International Organization for Standardization, 2009). The soil pH was determined after equilibrating soil suspensions with deionized  $\text{H}_2\text{O}$  at a liquid to solid ratio of 3 L  $\text{kg}^{-1}$  for 18 h, using a Radiometer PHM93 reference pH meter with a

**Table 1**  
Selected soil properties and annual fertilizer inputs.

	Ekebo	Fjärdingslöv	Högåsa	Kungsängen	Vreta Kloster
Location	55°59'N 12°52'E	55°24'N 13°14'E	58°30'N 15°27'E	59°50'N 17°40'E	58°30'N 15°30'E
Texture	Loam	Sandy loam	Loamy sand	Clay	Silty clay
pH	7.1	7.3	6.4	6.6	7.0
Organic C (%)	2.4	1.3	1.9	2.1	1.9
Fe <sub>ox</sub> (mmol kg <sup>-1</sup> )	40	32	57	170	35
Al <sub>ox</sub> (mmol kg <sup>-1</sup> )	81	34	78	63	71
Exchangeable Ca <sup>2+</sup> (cmol <sub>c</sub> kg <sup>-1</sup> )	7.9	11.3	3.8	20.8	21.3
N input (kg ha <sup>-1</sup> )	150	150	125	125	125
P and K input, A3 (kg ha <sup>-1</sup> )	0	0	0	0	0
P and K input, B3 (kg ha <sup>-1</sup> )	R	R	R	R	R
P input, C3 (kg ha <sup>-1</sup> )	R + 15	R + 15	R + 20	R + 20	R + 20
P input, D3 (kg ha <sup>-1</sup> )	R + 30				
K input, C3 (kg ha <sup>-1</sup> )	R + 40	R + 40	R + 50	R + 50	R + 50
K input, D3 (kg ha <sup>-1</sup> )	R + 80				

R = Replacement, i.e. P input that balances the P offtake. Fe<sub>ox</sub> and Al<sub>ox</sub> = oxalate-extractable Fe and Al. Values of exchangeable Ca<sup>2+</sup> are from Kirchmann (1991), Kirchmann et al. (1999), and Kirchmann et al. (2005). Values for pH, organic C, Fe<sub>ox</sub> and Al<sub>ox</sub> represent averages of all treatments in 2017; detailed results from all treatments are shown in Table S1. The fertilizer inputs represent annual averages over each crop rotation period.

GK2401C combined pH electrode. The organic carbon content was determined using a LECO CNS-2000 analyzer. Oxalate-extractable Fe, Al, and P (Fe<sub>ox</sub>, Al<sub>ox</sub>, and P<sub>ox</sub>) were extracted using an oxalate buffer at pH 3.0 for 4 h (van Reeuwijk, 1995), and subsequent analysis by ICP-OES using a Thermo ICAP 6300 instrument. Inorganic P in the oxalate extracts (P<sub>iox</sub>) was measured colorimetrically with the molybdate-blue method using a Seal AA3 Autoanalyzer, after modification of the reagent concentrations (Wolf and Baker, 1990). Oxalate extractions were also made for selected archived samples. Total P was measured after igniting the soil at 550 °C and subsequent extraction with 0.5 mol/L H<sub>2</sub>SO<sub>4</sub> for 16 h, followed by PO<sub>4</sub>-P determination using the malachite green method (Walker and Adams, 1958; Ohno and Zibilske, 1991). For all samples, acid ammonium lactate-extractable P (P<sub>AL</sub>) was determined using the method of Egnér et al. (1960), according to which 5 g dry soil was equilibrated for 1.5 h with 100 mL of a solution containing 0.1 mol/L ammonium lactate and 0.4 mol/L acetic acid at pH 3.75.

For the P-depleted A3 treatments of each soil, P sorption experiments were carried out for duplicate field plots according to Eriksson et al. (2016). Briefly, 2 g of soil was equilibrated with 30 mL solution containing 0.01 M NaNO<sub>3</sub> and 8 different levels with added NaH<sub>2</sub>PO<sub>4</sub> (0.15, 0.3, 0.6, 1.05, 1.5, 2.25, 3 and 4.5 mmol P kg<sup>-1</sup> soil, respectively). After 7 d of equilibration at 22 °C, the samples were centrifuged at 3000 rpm for 20 min. The pH of the supernatant was measured using a Radiometer PHM93 pH meter with a GK2401C combined pH electrode. The supernatant solution was filtered through a 0.2 µm single use filter (Acrodisc PF) before analysis of PO<sub>4</sub>-P (using a Seal Analytical AA3 Autoanalyzer with the molybdate blue method).

### 2.3. P K-edge XANES spectroscopy

P K-edge XANES results from the five sites have been reported earlier (Eriksson et al., 2016; Braun et al., 2019). However, to ensure

consistency with the current set of samples, new XANES measurements were performed for the samples collected in 2017 at BL-8 at the Synchrotron Light Research Institute (SLRI), Nakhon Ratchasima, Thailand (Klysubun et al., 2020). The methods for data acquisition have been described in detail earlier (Eriksson et al., 2016; Tuyishime et al., 2022) but are briefly summarized here. The X-ray photon energy was scanned by an InSb (111) double crystal monochromator giving a normalized beam flux of  $1.3 \times 10^9$  to  $3 \times 10^{11}$  photons s<sup>-1</sup> (100 mA)<sup>-1</sup>. The soil samples were homogenized, finely ground and sieved (to <50 µm) to minimize the effect of self-absorption. The samples were packed in stainless 1.5 cm<sup>2</sup> steel sample holder, which were covered with polypropylene X-ray film. The sample compartment was evacuated with helium (He) gas. The emitted fluorescence was measured using a solid-state 13-element Ge detector in the energy range of 2100–2320 eV. The maximum of the first derivative of the spectrum (E<sub>0</sub>) for the black P was set to 2145.5 eV for energy calibration. A variscite standard (E<sub>0</sub> = 2154.05 eV) was frequently measured to check any shift that occurred after every energy re-calibration. Between 4 and 8 scans were collected for each sample.

The spectra were merged, energy-corrected and normalized with the Athena code (Ravel and Newville, 2005) as detailed previously (Tuyishime et al., 2022). Each normalized sample spectrum was thereafter subjected to linear combination fitting (LCF) analysis using the LCF-LinEst code, which uses the Microsoft Excel LinEst function for optimization (Almkvist et al., 2010; Gustafsson, 2022). In the LCF, energy shifts were not permitted, the sum of weights (SOW) was not forced to 1, and a maximum of four standards was allowed in the output. 15 standards thought to represent the major P phases in the soils were included in the LCF, as described by Gustafsson et al. (2020). Outputs resulting in SOW < 0.95 and > 1.05 were not accepted. The best fit was chosen using the normalized residual sum-of-squares (NRSS) as the goodness-of-fit parameter:

$$NRSS = \frac{\sum_i [(data_i - fit_i)^2]}{\sum_i data_i^2} \quad (1)$$

Further, to determine the uncertainty of the obtained LCF weights, an uncertainty analysis (as described by Gustafsson et al., 2020) was performed using LCF-LinEst. For this, the 15 standards were divided into six species groups as follows: 1. *Soil organic P*: organic P from a Spodosol Oe horizon. 2. *Phosphate adsorbed to Al*: phosphate adsorbed to allophane, phosphate adsorbed to gibbsite, and phosphate adsorbed to Al(OH)<sub>3</sub>. 3. *Phosphate adsorbed to Fe*: phosphate adsorbed to ferrihydrite, phosphate adsorbed to goethite. 4. *Al phosphates*: variscite, amorphous AlPO<sub>4</sub>. 5. *Fe(III) phosphates*: strengite, amorphous FePO<sub>4</sub>. 6. *Ca phosphates*: apatite Taiba, hydroxyapatite, octacalcium phosphate (OCP), brushite, amorphous Ca phosphate.

### 2.4. The PBalD8 model. Mass balance terms

The PBalD8 (“Phosphorus mass balance model with diffusion to 8 compartments”) code (Gustafsson, 2023) was written in C# using Microsoft Visual Studio 2022. The mass balance was applied to the A horizons of the five studied sites for the period between the establishment of the experiment and 2017. The depth of the A horizon was assumed to be 0.25 m, which corresponds to the plow depth at these sites. The following mass balance constraint, serving as the core of the model, was used:

$$P_{dep} + P_{seed} + P_{fert} + P_{wea} = \Delta P_{labile} + \Delta P_{stable} + P_{off} + P_{appt} + P_{leach} \quad (2)$$

where the P sources on the left are: P<sub>dep</sub>, the atmospheric P deposition; P<sub>seed</sub>, the P applied in seeds at sowing; P<sub>fert</sub>, the P fertilizer input, and P<sub>wea</sub>, the amount of P weathered from apatite. The P sinks on the right are: ΔP<sub>labile</sub>, net change of the labile P pool; ΔP<sub>stable</sub> = net change of the stable P pool; P<sub>off</sub>, P removed by offtake; P<sub>appt</sub>, P precipitated as apatite, and P<sub>leach</sub>, P leached from the A horizon. The basic outline of the PBalD8

model is shown in Fig. 1. The model employed a time step of one week; thus the units used for all P sources and sinks were mol P wk<sup>-1</sup> m<sup>-3</sup> soil. The values of P<sub>dep</sub> and P<sub>seed</sub> were assumed not to change during the experiment (Table S1). Initially, P<sub>fert</sub> was given by known fertilizer inputs during the different rotation periods, as shown in Table 1.

Apatite weathering, P<sub>wea</sub>, was assumed to occur when the soil solution was undersaturated with respect to apatite, and with Ca phosphate contents constrained by P K-edge XANES spectroscopy. To calculate the saturation status with respect to hydroxyapatite, a log \*K<sub>s</sub> value of {Ca<sup>2+</sup>}<sup>5</sup>{PO<sub>4</sub><sup>3-</sup>}<sup>3</sup>{H<sup>+</sup>} = -44.3 at infinite dilution was used (Gustafsson, 2022). Further, an ionic strength of 0.005 M was assumed and dissolved Ca<sup>2+</sup> was estimated using values given in Table S1. P<sub>wea</sub> was calculated using the Profile model (Sverdrup and Warfvinge, 1993) using the following main equation:

$$r = k_{H^+} \cdot \frac{\{H^+\}^{n_H}}{f_H} + \frac{k_{H_2O}}{f_{H_2O}} + k_{CO_2} \cdot P_{CO_2}^{n_{CO_2}} \quad (3)$$

where *r* is the apatite weathering rate (kmol<sub>c</sub> m<sup>-2</sup> s<sup>-1</sup>), *k*<sub>H<sup>+</sup></sub> and *k*<sub>H<sub>2</sub>O</sub> are rate coefficients for the reaction with H<sup>+</sup> and H<sub>2</sub>O, respectively (m s<sup>-1</sup>), *n*<sub>H</sub> and *n*<sub>CO<sub>2</sub></sub> are reaction orders of individual reactions, *P*<sub>CO<sub>2</sub></sub> is the partial CO<sub>2</sub> pressure (atm), while *f*<sub>H</sub> and *f*<sub>H<sub>2</sub>O</sub> are retardation factors (“brakes”). Values of all coefficients, as well as the exact definition of the retardation factors, are detailed in Sverdrup and Warfvinge (1993). The *P*<sub>CO<sub>2</sub></sub> was assumed to be 0.005 atm (Table S1). To calculate P<sub>appt</sub>, i.e. Ca phosphate precipitation, which was found to be important at the Fjärdingslöv site, it was acknowledged that a large supersaturation is required to form appreciable amounts (e.g., Johansson and Gustafsson, 2000). Here a log IAP (ion activity product) = -37.8 for hydroxyapatite at infinite dilution was used, which provided a reasonable fit to the Fjärdingslöv data, c.f. the Results section. The amount of P leaching,

P<sub>leach</sub>, was constrained from the adsorption/diffusion model and from the values of the remaining terms in Eq. (2).

### 2.5. PBalD8 model. Adsorption and diffusion to/from slow pools

The Freundlich equation was used to describe P adsorption/desorption, while Fick’s first law with a time step of one week was used for modelling the mass transfer of P from the soil solution to the ‘stable’ pools and vice versa. For porous media, Fick’s first law can be written as (e.g. Schackelford and Daniel, 1991):

$$J = -D_e \cdot \theta \cdot \tau \cdot \frac{\partial C}{\partial X} \quad (4)$$

where *J* = the flux density of P from the bulk solution to the pore domain (mol m<sup>-2</sup> week<sup>-1</sup>), *D<sub>e</sub>* = effective dispersion coefficient of P (m<sup>2</sup> week<sup>-1</sup>), *C* = concentration of the solute (mol m<sup>-3</sup>), *θ* is the volumetric water content (m<sup>3</sup> m<sup>-3</sup>), *τ* is the matrix tortuosity factor, which is a function of soil physical properties such as the particle-size distribution (e.g., Nye and Tinker, 1977), and *X* = length (m). Equation (4) requires knowledge of the external surface area of the sorbent to be practically useful. Also, the diffusion length Δ*X* is typically not a known quantity. For these reasons, it is convenient to convert *D<sub>e</sub>* to a soil-specific “permeability”, i.e., an effective diffusion coefficient where Δ*X* is not explicitly quantified. Thus, Eq. (4) was rewritten to consider the change of the stable P pool during one week:

$$\Delta P_{stable} = P_s \cdot \theta \cdot (C_{bulk} - C_{solid}) \quad (5)$$

where the unit of Δ*P*<sub>stable</sub> is mol week<sup>-1</sup> m<sup>-3</sup> soil, while *C*<sub>bulk</sub> is dissolved P in the soil solution (mol m<sup>-3</sup>) and *C*<sub>solid</sub> is the dissolved P on the inside of the diffusion barrier (mol m<sup>-3</sup>). *P<sub>s</sub>*, the soil-specific permeability

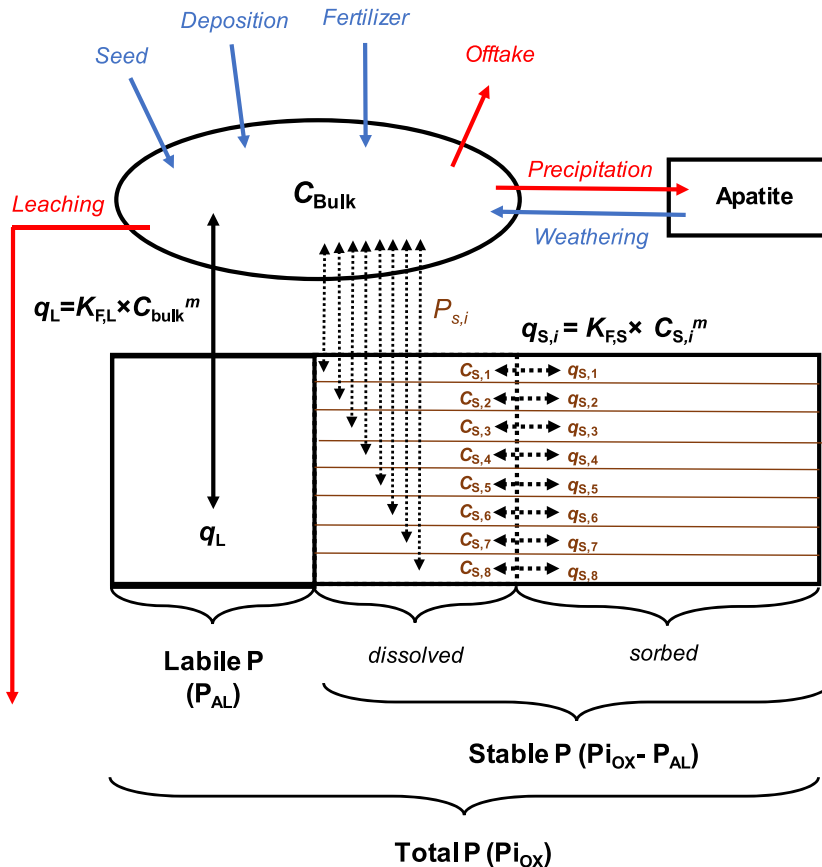


Fig. 1. Schematic illustration of the PBalD8 model, showing all P fluxes considered and the division between the two sorbed P pools, labile P and stable P, where the latter is divided into 8 compartments having an equal number of P sorption sites.

(week<sup>-1</sup>), is related to the diffusion coefficient  $D_e$  as follows:

$$P_s = \frac{D_e \cdot \tau \cdot A}{\Delta X} \quad (6)$$

where  $A$  is the external surface area of the sorbent ( $\text{m}^2 \text{m}^{-3}$  soil). In Eq. (5),  $\theta$  converts from soil solution basis to soil volume basis; however, in the modelling approach used here, temporal variations are not considered, i.e.,  $\theta$  is constant. It is likely that the soil sorbents contain aggregates of Fe and Al hydrous oxides that differ in terms of  $\Delta X$  and consequently in  $P_s$ . Here, we assume that the variability of  $P_s$  can be described using a rectangular distribution consisting of 8 discrete compartments of equal size in terms of the number of P sorption sites:

$$\log P_{s,i} = \log P_{s,1} + (i - 1) \cdot \Delta \log P_s; \quad i = 1, 2, 3, 4 \dots 8 \quad (7)$$

where  $P_{s,1}$  represents the permeability of the first compartment, which is the 'fastest' stable P pool in terms of sorption/desorption).  $\Delta \log P_s$  determines the width of the rectangular distribution of permeabilities. These two parameters collectively define the entire range of permeabilities within the soil matrix. This approach bears similarity to the method used to address heterogeneous binding sites in the WHAM and SHM organic complexation models (Tipping, 1994; Gustafsson, 2001). Within each compartment and also on the external surface in direct contact with the soil solution (referred to as the labile P), the relationship between dissolved and sorbed P is governed by the Freundlich equation:

$$q = K_F \cdot C^m \quad (8)$$

where  $q$  represents the sorbed P in a compartment ( $\text{mol kg}^{-1}$ ),  $C$  stands for the dissolved P concentration ( $\text{mol L}^{-1}$ ), while  $K_F$  and  $m$  are coefficients. The P sorption strength is assumed to be identical for labile P and for all stable P compartments, meaning that values for  $m$  are assumed to be the same. However,  $K_F$  is proportional to the number of sites within a compartment. This relationship is governed by  $f_{\text{active}}$ , which is the fraction of sites that react quickly (i.e., in direct contact with the soil solution), and  $f_i$ , representing the fraction of sites in each slow compartment, where  $f_i = (1 - f_{\text{active}})/8$ . In the current model implementation,  $P_{\text{AL}}$  is assumed to represent the labile pool of P, whereas  $P_{\text{IOX}}$ , i.e., oxalate-extractable inorganic P, is assumed to represent the amount of geochemically active P (c.f. Results). At  $t = 0$ , i.e., at the start of the simulation, a steady state between the bulk solution and the porous solids is assumed such that  $C_{\text{bulk}} = C_{i,1-8}$ . Under these conditions,  $f_{\text{active}}$  is approximated as follows:

$$f_{\text{active}} = \frac{P_{\text{AL}}}{P_{\text{IOX}}} \quad (9)$$

## 2.6. Model optimization

Model optimization resulted in values of  $\log P_{s,1}$  and  $\Delta \log P_s$  for each individual soil using PEST (Doherty, 2010), with  $P_{\text{AL}}$  and  $P_{\text{IOX}}$  as fitting variables and input parameter values detailed in Table S1. Initially, values of  $P_{\text{off}}$  and  $P_{\text{fert}}$  were constrained by measured values of P offtake and known P fertilizer additions during the experiments. However, this led to very poor fits, both in the P-depleted treatments (A3, see Table 1) where fitted  $P_{\text{IOX}}$  and  $P_{\text{AL}}$  with time became much lower than those measured, and in some of the high-fertilizer C3 and D3 treatments, where the opposite occurred. To improve the fits in the P-depleted treatments, it was assumed that crops increasingly took up P from deeper soil layers when dissolved P in the A horizon was low (c.f. Results and Discussion section). We used the following brake function (McGivney et al., 2019) to limit P offtake from the A horizon:

$$f_{\text{upt}} = \frac{[\text{P}]^n}{[\text{P}]^n + c^n} \quad (10)$$

where  $[\text{P}]$  is dissolved P in the A horizon soil solution ( $\mu\text{mol L}^{-1}$ ),

whereas the values of  $n$  and  $c$  were set to 1.5 and 0.5, respectively. This combination of values appeared to provide a reasonable description of the brake effect in all soils, c.f. the Results section. Hence, the modelled P offtake was calculated as  $P_{\text{off}} \times f_{\text{upt}}$ . We also introduced a coefficient  $f_{\text{fert}}$  to modify P fertilizer inputs where this was necessary for satisfactory model fits, as follows:

$$P_{\text{fert,model}} = f_{\text{fert}} \times P_{\text{fert,nominal}} \quad (11)$$

where  $P_{\text{fert,nominal}}$  is the fertiliser input of P according to historical records, whereas  $P_{\text{fert,model}}$  is the P fertiliser input finally used in the model. Adjustment of  $f_{\text{fert}}$  (from the initial value of 1) was found to be necessary in 3 of 5 soils, where  $f_{\text{fert}}$  was set to 0.8 (Ekebo and Kungsängen) or 0.7 (Högåsa).

## 3. Results and Discussion

### 3.1. Phosphate sorption and phosphorus extractability

The data from the P sorption experiments were fitted with the Freundlich equation after logarithmic transformation using the constraint that the amount of sorbed P ( $Q$  in Eq. (8)) was the sum of initially bound P and the amount bound during the 7-d experiment. Due to the short time scale of the batch experiments, the initially bound P was assumed to be represented by the 'fast'  $P_{\text{AL}}$  pool. As Fig. S1 shows, very good fits to the P sorption data were obtained for the P-depleted A3 treatment, with values of the Freundlich  $m$  non-ideality parameter ranging from 0.299 to 0.478, which is similar in magnitude to  $m$  values obtained or used in other studies (Börling et al., 2001; Gustafsson et al., 2012; Eriksson et al., 2016). The averaged parameters, shown in Table S1, were used for all fertilizer treatments within the same site during P<sub>BALD8</sub> modelling.

The data on extracted P were consistent with those reported earlier for these sites (e.g. Bergström et al., 2015; Eriksson et al., 2016; Braun et al., 2019), i.e., extractable P increased in the strongly fertilized C3 and D3 treatments, while it decreased in the P-depleted A3 treatments (Table S1). As previously observed for these and other soils, oxalate-extractable P ( $P_{\text{OX}}$  and  $P_{\text{IOX}}$ ), as well as total P, changed considerably more than  $P_{\text{AL}}$ , indicating that diffusion to/from stable P pools was an important long-term process governing the storage and release of P (Eriksson et al., 2016; Amery et al., 2021). When  $P_{\text{OX}}$  was divided into inorganic P (i.e.  $P_{\text{IOX}}$ , the fraction of  $P_{\text{OX}}$  that was determined colorimetrically) and organic P (calculated as  $P_{\text{OX}} - P_{\text{IOX}}$ ), it was found that  $P_{\text{IOX}}$  responded strongly to different P fertilizer inputs, while oxalate-extractable organic P did not (Fig. S2). In fact, when extracted P was expressed relative to that observed in the P-depleted A3 treatment, very similar results were obtained for  $P_{\text{IOX}}$  as for total P (Fig. 2), suggesting that the changes in P status in response to different fertilizer inputs could be fully explained by changes in  $P_{\text{IOX}}$ , whereas P species not included in  $P_{\text{IOX}}$  (e.g., organic P, crystalline Ca phosphate) did not change with fertilizer input. The resulting changes in labile and stable P between 1963/67 and 2017 are shown in Fig. S3. The finding that inorganic P, but not organic P, responds to different fertilization regimes is not novel (Ahlgren et al., 2013; Bergström et al., 2015; Eriksson et al., 2016). However, it is of particular interest that  $P_{\text{IOX}}$  can be used to investigate these responses, as  $P_{\text{IOX}}$  extracts a smaller proportion of total P than other methods that were previously used to determine reactive P, such as  $P_{\text{OX}}$  or acid-digestible P; hence, differences between treatments can be determined with a greater degree of confidence.

### 3.2. Phosphorus speciation according to XANES spectroscopy

The P K-edge XANES speciation results, normalized with respect to acid-digestible P, are shown in Fig. 3. As only one plot per treatment was studied, the results cannot be used to infer treatment effects on P speciation. However, the general trends in P speciation are consistent

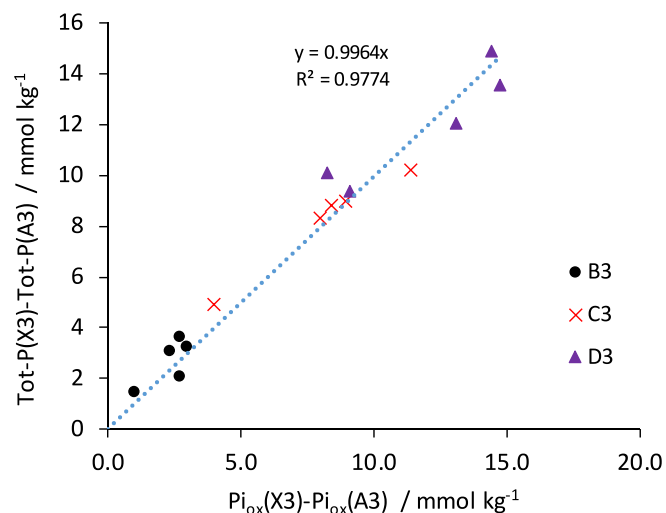


Fig. 2. The differences between total P determined in the B3, C3 and D3 treatments and total P in the A3 treatments (averages from each site in 2017) plotted as a function of the corresponding differences between oxalate-extractable inorganic P ( $P_{i_{ox}}$ ).

with those found for an earlier set of samples from the sites (Eriksson et al., 2016; Braun et al., 2019). That is, while Fe- and Al-bound P increased in response to fertilization, organic P remained largely unchanged, in agreement with the trends in extracted P fractions. Additionally, for the Fjärdingslöv site, there seemed to be an increase in Ca phosphate in response to the highest fertilization levels. This finding is also consistent with earlier research that involved evidence from pH-dependent P dissolution experiments (Eriksson et al., 2016).

### 3.3. Mass balance modelling

The final model, which had been adjusted in ways that are explained below, was able to provide good fits to the  $P_{AL}$  and  $P_{i_{ox}}$  data (for fitted parameters, see Table 2; for model fits, see Fig. 4). However, the fitted values of  $\log P_{s,1}$  and  $\Delta \log P_s$  were not well constrained; different combinations of the two often led to very similar fit qualities. Almost equally good fits could be obtained by fixing  $\log P_{s,1}$  to a common value of  $-0.15$  for all soils, optimizing only  $\Delta \log P_s$  (Table 2). The two models are referred to as models A and B, respectively. Due to the smaller number of adjusted parameters, model B was selected for further data treatment and analysis. To constrain  $\log P_{s,1}$  and  $\Delta \log P_s$  further, an even wider variation of adsorbed P would be needed. Furthermore, there was no evident strong relationship between the fitted  $\log P_{s,1}$  and  $\Delta \log P_s$  values on the one hand, and the properties of the 5 soils on the other. Nevertheless, it is worth noting that Fjärdingslöv exhibited the lowest  $\Delta \log P_s$  value, when model B was used. This observation could potentially be associated with the prediction of calcium phosphate precipitation in the most heavily fertilized treatment, although the underlying reason for this phenomenon remains unclear. A more extensive data set, with additional soils being analysed, would probably be necessary to establish any significant relationships between the permeability parameters and soil properties.

For the P-depleted A3 treatments, the PbalD8 model was not able to yield acceptable fits to the  $P_{AL}$  and  $P_{i_{ox}}$  data without the use of the “brake” function of Eq. (10). The measured P offtake was too high to explain the relatively modest decrease in  $P_{AL}$  and  $P_{i_{ox}}$  that was observed, at least with the input parameters and assumptions used. Hence Eq. (10) was implemented, with values of  $n$  and  $c$  set to 1.5 and 0.5, respectively. This resulted in large reductions in the modelled P offtake of the A3 treatments, particularly for the Fjärdingslöv and Vreta Kloster sites (Fig. S4). With the modified P offtake, the temporal development of  $P_{AL}$  and  $P_{i_{ox}}$  could be successfully captured in all sites (Fig. 4).

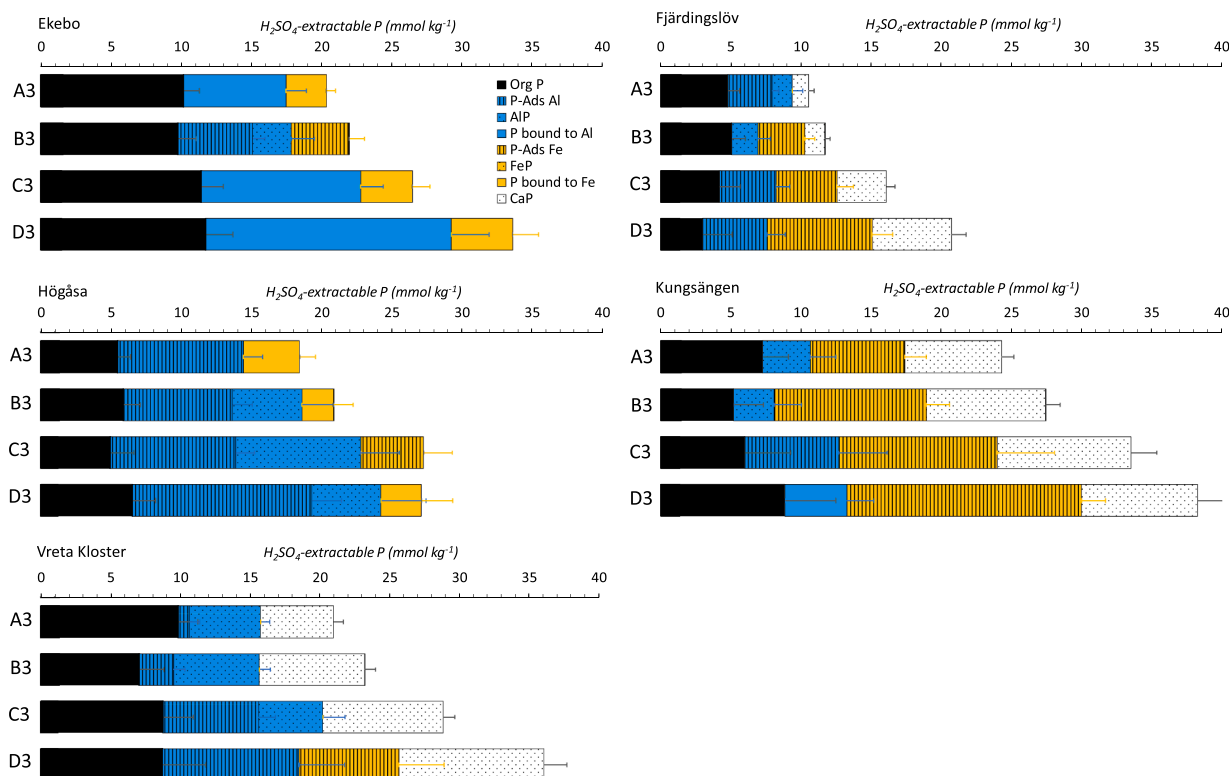


Fig. 3. Phosphorus speciation according to P K-edge XANES spectroscopy, where the mean weights of P fractions from LCF analysis has been recalculated to fractions of pseudo-total soil ( $H_2SO_4$ -extractable) P. For each fraction, the uncertainty is shown. See Table S3, S4 and S5 for detailed results.

**Table 2**  
Optimised parameter values and goodness-of-fit for the PBalD8 model.

Site	Treatment	$f_{fert}$	Model A			Model B		
			$\log P_{s,1}$	$\Delta \log P_s$	PEST R	$\log P_{s,1}$	$\Delta \log P_s$	PEST R
Ekebo	A3	–	–0.8	0	0.9758	–0.15	–0.14	0.9750
	B3	0.85						
	C3	0.8						
	D3	0.8						
Fjärdingslöv	A3	–	–0.7	–0.46	0.9759	–0.15	–0.65	0.9759
	B3	1						
	C3	1						
	D3	1						
Högåsa	A3	–	1.0	–0.33	0.9841	–0.15	0	0.9836
	B3	0.85						
	C3	0.7						
	D3	0.7						
Kungsängen	A3	–	–0.1	–0.13	0.9950	–0.15	–0.11	0.9950
	B3	0.85						
	C3	0.8						
	D3	0.8						
Vreta Kloster	A3	–	1.1	–0.77	0.9860	–0.15	–0.44	0.9859
	B3	1						
	C3	1						
	D3	1						

Note: A3, B3, C3 and D3 represent the different fertiliser levels (Table 1),  $\log P_{s,1}$  and  $\Delta \log P_s$  are permeability coefficients as defined in Eq. (7), and  $f_{fert}$  is a factor modifying the amount of fertiliser input to the A horizon, Eq. (11). Values in italics were fixed during optimization. PEST R is the goodness-of-fit value reported by PEST (Doherty, 2010). For Fjärdingslöv, results are shown for the scenario where apatite is precipitated.

The necessity to include a relationship such as Eq. (10) can be explained in two fundamentally different ways: 1) due to tillage and erosion, soil particles from adjacent P-fertilized plots were mixed into the A horizons of the A3 treatment plots (Sibbesen et al., 2000). This means that the actual P input was much larger than what was considered from atmospheric deposition and sowing only. Alternatively, 2) as soil solution P became lower, crops may have taken up a larger fraction of P from the subsoil, which was not considered in the original mass balance. Support for this observation comes from other long-term P-depletion experiments (e.g., Zicker et al., 2018; Seidel et al., 2021; Siebers et al., 2021), as well as from the mass balance modeling study of Messiga et al. (2015).

Both of the above explanations may be correct to some extent. However, with the available data, it is not possible to determine which is the most important. We note that in most sites,  $P_{AL}$  declined more rapidly in the beginning and less towards the end of the experimental period (Fig. 4), which supports a model in which a progressively larger fraction of P is taken up from the subsoil with time, as suggested by Eq. (10). This is in contrast to a model in which a certain fraction of P fertilizer is unintentionally spread to the A3 plots every time PK fertilizer is applied to the adjacent plots. Therefore, in Table 3, where the mass balance terms are presented, the P outputs have been decreased by presenting the modeled P offtake (“adjusted P offtake”), rather than increasing the P inputs through unintentionally spread P fertilizer.

For the P-fertilized treatments B3, C3, and D3, it was possible to obtain satisfactory PBalD8 model fits without any adjustments of input parameters for the Vreta Kloster site, but not for the other sites. The satisfactory fits to  $P_{AL}$  and  $Pi_{OX}$  at the Vreta Kloster site suggest that the input parameters may have been correctly assessed, which likely makes the mass balance terms of Table 3 less uncertain than for the other sites. However, for the Ekebo, Högåsa, and Kungsängen sites, the use of nominal (i.e., unchanged) P fertilizer inputs resulted in too strong accumulations of soil P as  $Pi_{OX}$ , particularly for the C3 and D3 treatments. When  $f_{fert}$  was set to 0.8 (Ekebo and Kungsängen) or 0.7 (Högåsa), much better fits were obtained, implying that the fertilizer P input to the A horizon was only 80 % or 70 % of the nominal one according to the experimental protocol. Again, this discrepancy can be due to several causes. First, the fertilizer input may have been lower than intended. Second, some of the fertilizer may have unintentionally spread to adjacent plots, aligning with the findings of Sibbesen et al. (2000).

Third, some A horizon material may have become mixed into deeper mineral soil layers, resulting in a greater export of P from the A horizon to the subsoil than could be accounted for solely by leaching. This phenomenon might have occurred, for example, due to bioturbation or deep tillage, both of which were discussed as factors influencing the relative P enrichment observed at depths of 25–50 cm in Danish agricultural soils (Rubaek et al., 2013). Considerable downward movement of P from the A horizon to deeper soil strata was also observed for other soils (de Bolle et al., 2013; van der Bom et al., 2019; Siebers et al., 2021) although in these cases, no attempt was made to differentiate the effects of leaching from those of physical mixing. Nevertheless, it is evident that in certain soils, very little P movement is observed below a depth of 30 cm (Azeez et al., 2020; Siebers et al., 2021), which led Siebers et al. (2021) to hypothesize that deep soil mixing is strongly site-dependent, occurring in some soils but not in others. However, in the absence of subsoil results, we cannot definitely determine which of these three explanations is the most likely.

For the Fjärdingslöv soil, the PBalD8 model performed very well in describing the development of  $P_{AL}$  and  $Pi_{OX}$  in the B3 and C3 treatments with  $f_{fert}$  set to 1, i.e., with P fertilizer input equal to the nominal one (Fig. 4, Table 2). However, for the highest fertilization level (D3), the model produced large underestimations of  $P_{AL}$  as well as  $Pi_{OX}$  in the latter half of the experimental period (data not shown). A likely explanation is that non-crystalline, oxalate-extractable Ca phosphate had been formed in the D3 plots, as was shown by Eriksson et al. (2016) and confirmed using XANES in this study. Hence, we allowed for Ca phosphate precipitation to occur (see Methods section) using the assumption that all the accumulated Ca phosphate was extractable with oxalate. As it is likely that at least some of the neoformed Ca phosphate is extracted also by acid ammonium lactate (Eriksson et al., 2016), we fitted the percentage of formed Ca phosphate extracted as  $P_{AL}$  and arrived at a value of 65 %. With these modifications to the original model, and with  $f_{fert}$  set to 1, we were able to obtain a very good fit to the data (Fig. 4). According to the model, 559 kg P ha<sup>-1</sup> had been precipitated as Ca phosphate, which is equivalent to 4.3 mmol P kg<sup>-1</sup> using the parameter values of Table S2. This value is close to the relative accumulation of Ca-P in the investigated D3 plot as compared to the A3 and B3 plots, according to P K-edge XANES (Table S3).

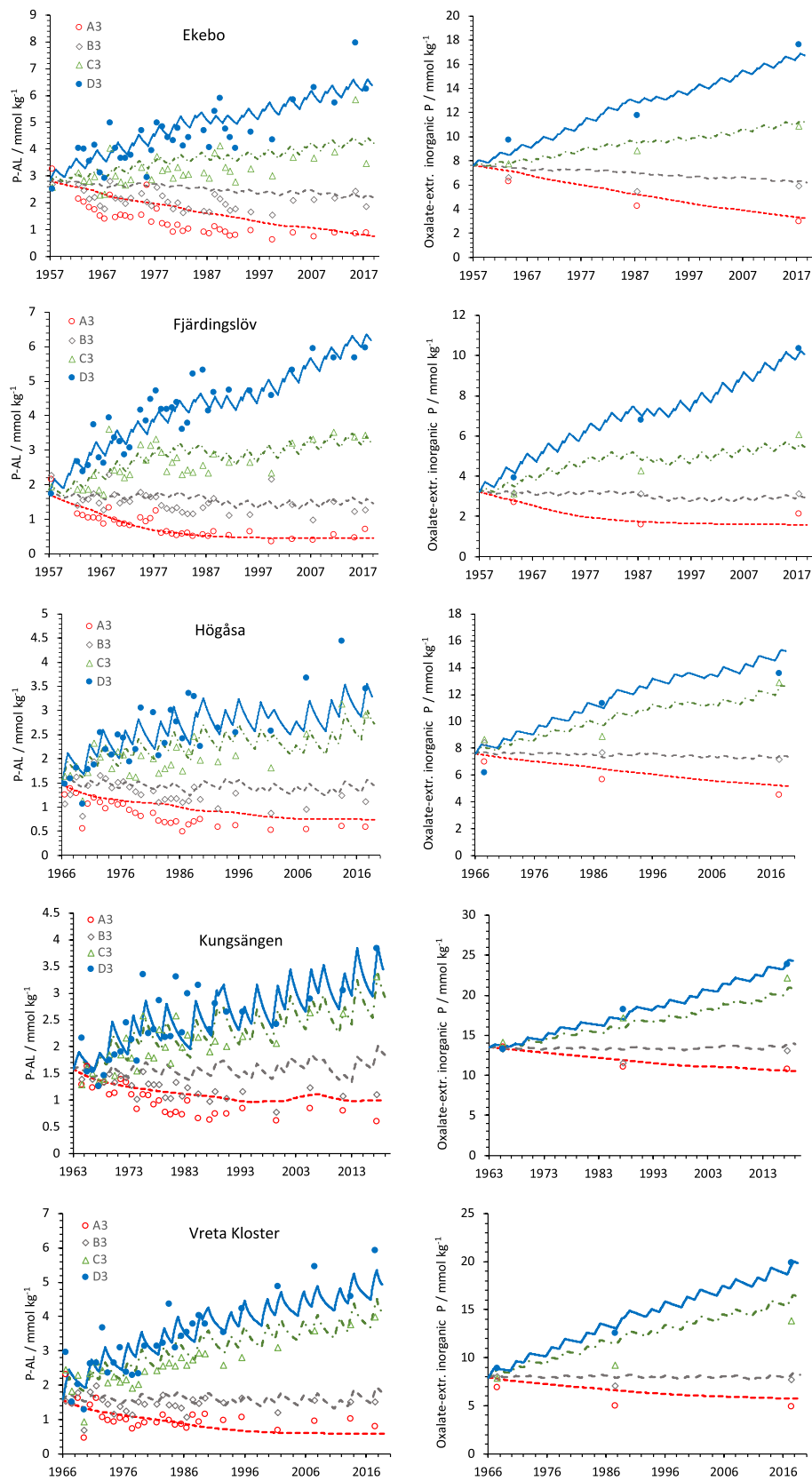


**Fig. 4.** Development of  $P_{AL}$  and  $Pi_{OX}$  in all treatments over the experimental period since the start of the fertility experiments. Each data point represents an average of two duplicate plots. A3, B3, C3 and D3 represent the different fertiliser levels, c.f. Table 1. The lines are PBalD8 model fits using the optimised parameters of model B shown in Table 2.

**Table 3**  
Model-estimated mass balances of phosphorus (kg P ha<sup>-1</sup>).

Site, time	Treatment	Inputs	Outputs						
		Atmosphere + Seeds	Fertilization	Weathering	Sorption(labile P)	Sorption (stable P)	Apatite precipitation	Adjusted offtake	Leaching
Ekebo 1957–2017	A3	36	0	0	-230	-256	0	497	25
	B3	36	548	0	-72	-84	0	686	54
	C3	36	1319	0	154	237	0	845	121
	D3	36	2122	0	385	619	0	914	240
Fjärdingslöv 1957–2017	A3	36	0	5.8	-164	-48	0	241	12
	B3	36	921	0	-34	-10	0	923	78
	C3	36	1866	0	184	89	0	1054	576
	D3	36	2803	0	200	104	561	1083	892
Högåsa 1966–2017	A3	30	0	0	-79	-179	0	281	6.3
	B3	30	456	0	-2.9	-19	0	493	14
	C3	30	1139	0	133	398	0	600	38
	D3	30	1531	0	185	628	0	695	54
Kungsängen 1963–2017	A3	33	0	131	-60	-242	0	456	9.1
	B3	33	555	114	26	16	0	641	19
	C3	33	1385	98	136	608	0	729	44
	D3	33	1777	85	178	912	0	747	58
Vreta Kloster 1966–2017	A3	30	0	65	-110	-135	0	335	5.4
	B3	30	744	0	18	13	0	715	28
	C3	30	1959	0	275	656	0	830	228
	D3	30	2498	0	365	948	0	825	390

### 3.4. Implications for the role of different P sources and sinks

As expected, the mass balance model showed P input to be dominated by fertilizer input in the fertilized treatments, and by desorption of previously sorbed P in the unfertilized A3 treatments (Table 3). By contrast, phosphorus input through atmospheric deposition and sowing were insignificant P sources to these agricultural soils (Table 3). The Profile weathering submodel indicated apatite weathering to be an additional significant long-term P source in the Kungsängen soil and in the P-depleted Vreta Kloster soil. If this is correct, this process can significantly delay the decrease of P<sub>AL</sub> in the P-depleted plots of these sites. In the other sites this process is not predicted to be important, due to the absence of apatite or because of the higher pH and/or (in the case of the fertilized Vreta Kloster treatments) higher dissolved P. To our knowledge, this is the first time the contribution to P from weathering has been quantified in a mass balance model for agricultural soils, although the obtained results cannot at present be verified with available field data.

As for the sinks, P offtake dominated, with P sorption as an important additional sink in the fertilized treatments (Table 3). The relative roles of offtake and sorption differed depending on the soil. Over the experimental period considered, sorption was a more powerful P sink than offtake in the heavily fertilized C3 and D3 treatments of the Kungsängen and Vreta Kloster sites. For Ekebo and Högåsa, the two sinks were of the same magnitude, at least in the D3 treatments. However, in Fjärdingslöv the role of sorption was much smaller, although a large part of the added P was bound as Ca phosphate in the D3 plots. These differences are to a significant extent due to differences in P sorption characteristics as manifested by the P isotherm results (Fig. S1), but the relative significance of other sources and sinks is also important in this respect.

In some of the soils, leaching was suggested to be an important additional P sink. The model predicted Fjärdingslöv D3 to be the soil with the highest leaching, i.e., 892 kg P ha<sup>-1</sup> over 61 years. This corresponds to a mean dissolved P concentration of  $\approx 3.7$  mg P L<sup>-1</sup>. This is clearly higher than the P concentrations measured by Svanbäck et al. (2013) in lysimeter experiments with the same soil, with P  $\approx 1$  mg P L<sup>-1</sup>. For the D3 treatments of Högåsa and Kungsängen, the model suggested lower P leaching (Table 3), i.e. 54 and 58 kg P ha<sup>-1</sup>, which corresponds to mean dissolved P  $\approx 0.5$  mg P L<sup>-1</sup> (Högåsa) or 0.3 mg P L<sup>-1</sup> (Kungsängen). Again, dissolved P, as measured by Svanbäck et al. (2013), was lower. There could be several reasons for these discrepancies. One possibility is that our adsorption experiments were carried

out using 0.01 mol L<sup>-1</sup> NaNO<sub>3</sub> as a background electrolyte, while the real solution conditions were different. For example, if dissolved Ca<sup>2+</sup> is higher in the field than in the experiment, the resulting surface potential of the Fe- and Al-containing sorbents may be more favourable towards P adsorption.

### 3.5. Future use of the model

A dynamic mass balance model, such as the one used here, could theoretically predict fertilizer requirements in a wide variety of soils considering also the effect of sorption to/desorption from stable P pools, if sufficient information on fertilization history, P offtake, and P sorption characteristics can be assembled. Further, the model could be used to improve the descriptions of P chemistry in larger ecosystem models such as ICECREAM to predict P leaching (Tattari et al., 2001; Radcliffe et al., 2015), and in Earth system models such as ELM-FUN (Braghiere et al., 2022). The model fits shown here indicate that this might be possible, but at the same time, our exercise also highlights a number of knowledge gaps that need to be filled in order to arrive at a reliable model tool. First, the role of the subsoil concerning crop uptake of P and the extent of physical mixing with A horizon material needs to be more adequately known. This is particularly important in a P depletion scenario, in which it is obvious that a simple mass balance approach, considering only sinks and sources within the A horizon, is unsuccessful. Second, the extent of leaching needs to be more accurately determined to constrain the mass balance models, and adsorption experiments to establish sorption properties may need to be carried out under conditions that more closely reflect field conditions. In many long-term field experiments, detailed information on P leaching from the A horizon is not available, which contributes to significant uncertainties in the P mass-balance determinations. Third, the current study was conducted in systems without livestock, utilizing mineral fertilizer as the primary fertilizer source. In systems where manure is employed, the cycling of organic phosphorus may potentially become of greater significance. Fourth, as it is clear that slow sorption/desorption of P is key to the understanding of long-term soil responses to P fertilization (or the absence thereof), solid-state diffusion processes need to be more adequately understood.

## 4. Conclusions

Both labile and stable soil pools of P significantly contributed to P sorption and desorption in the A horizons of five agricultural soils

subject to different fertilization treatments over 50–60 years. In the most heavily fertilized treatment (D3), the modelled value of the labile P pool increased by up to 385 kg P ha<sup>-1</sup> (Ekebo), while it decreased by a maximum of 230 kg P ha<sup>-1</sup> in the treatment without P fertilizer (also at Ekebo). The corresponding figures for the stable P pool were 948 kg P ha<sup>-1</sup> in the D3 treatment (Vreta Kloster) and 256 kg P ha<sup>-1</sup> in the P-depleted A3 treatment (Ekebo). In addition, calcium phosphate precipitation occurred in the highest P fertilizer treatment of one soil (Fjärdingslöv), adding 560 kg P ha<sup>-1</sup> to the total sorbed P. In the PBalD8 mass balance model, the amounts of P removed through harvest had to be decreased for the P-depleted treatments, compared to the measurements. This was interpreted as evidence for P uptake from deeper soil horizons as the surface horizon became increasingly P-depleted. Moreover, in 3 out of 5 soils, the amount of added fertilizer had to be decreased compared to known values, possibly because of bioturbation and mixing with deeper soil horizons during the course of the experiments, although other factors cannot be excluded. These findings highlight the need to consider also deeper mineral soil horizons to get a more complete picture of the mass balance in agricultural soils. Further, in a few cases, the model predicted mineral weathering to be a significant part of the mass balance. Even though the model produced results that were consistent with the P K-edge XANES results obtained, its predicted leaching estimates were higher than previous observations, which suggests that the model can be further improved.

#### CRedit authorship contribution statement

**Jon Petter Gustafsson:** Conceptualization, Formal analysis, Investigation, Methodology, Software, Writing – original draft, Writing – review & editing. **Florian Barbi:** Conceptualization, Formal analysis, Investigation, Methodology, Software, Writing – original draft, Writing – review & editing. **Sabina Braun:** Conceptualization, Data curation, Formal analysis, Investigation, Methodology, Writing – original draft, Writing – review & editing. **Wantana Klysubun:** Methodology, Resources, Writing – original draft, Writing – review & editing. **Gunnar Börjesson:** Data curation, Investigation, Resources.

#### Declaration of competing interest

The authors declare the following financial interests/personal relationships which may be considered as potential competing interests: Jon Petter Gustafsson reports financial support was provided by Foundation for Agricultural Research.

#### Data availability

Data will be made available on request.

#### Acknowledgments

This work was funded by Swedish Farmers' Foundation for Agricultural Research (Stiftelsen Lantbruksforskning; grant no. O-15-23-311). We thank Elin Ljunggren and Agnieszka Renman for support during the phosphate extraction and analysis. The Synchrotron Light Research Institute (Nakhon Ratchasima, Thailand) is acknowledged for beamtime and experimental support.

#### Appendix A. Supplementary data

Supplementary data to this article can be found online at <https://doi.org/10.1016/j.geoderma.2023.116727>.

#### References

- Ahlgren, J., Djodjic, F., Börjesson, G., Mattsson, L., 2013. Identification and quantification of organic phosphorus forms in soils from fertility experiments. *Soil Use Manage.* 29 (Suppl. 1), 24–35. <https://doi.org/10.1111/sum.12014>.
- Almkvist, G., Boye, K., Persson, I., 2010. K-edge XANES analysis of sulfur compounds: an investigation of the relative intensities using internal calibration. *J. Synchrotron Rad.* 17, 683–688. <https://doi.org/10.1107/S0909049510022946>.
- Amery, F., Vandecasteele, B., D'Hose, T., Nawara, S., Elsen, A., Odeurs, W., Vandendriessche, H., Arlotti, D., McGrath, S.P., Cougnon, M., Smolders, E., 2021. Dynamics of soil phosphorus measured by ammonium lactate extraction as a function of the soil phosphorus balance and soil phosphorus. *Geoderma* 385, 114855. <https://doi.org/10.1016/j.geoderma.2020.114855>.
- Azeez, M.O., Christensen, J.T., Ravnkov, S., Heckrath, G.J., Labouriau, R., Christensen, B.T., Rubæk, G.H., 2020. Phosphorus in an arable coarse sandy soil profile after 74 years with different lime and P fertilizer applications. *Geoderma* 376, 114555. <https://doi.org/10.1016/j.geoderma.2020.114555>.
- Barrow, N.J., 1983. A mechanistic model for describing the sorption and desorption of phosphate by soil. *J. Soil Sci.* 34, 733–750. <https://doi.org/10.1111/j.1365-2389.1983.tb01068.x>.
- Barrow, N.J., Shaw, T.C., 1975. The slow reactions between soil and anions: effect of time and temperature on the decrease in phosphate concentrations in the soil solution. *Soil Sci.* 119, 167–177.
- Bergström, L., Kirchmann, H., Djodjic, F., Kyllmar, K., Ulén, B., Liu, J., Andersson, H., Aronsson, H., Börjesson, G., Kynkänmi, P., Svanbäck, A., Villa, A., 2015. Turnover and losses of phosphorus in Swedish agricultural soils: long-term changes, leaching trends, and mitigation measures. *J. Environ. Qual.* 44, 512–523. <https://doi.org/10.2134/jeq2014.04.0165>.
- Bertilsson, G., Rosenqvist, H., Mattsson, L., 2005. Fosforgödsling och odlingsekonomi med perspektiv på miljömål (in Swedish). Swedish Environmental Protection Agency, Stockholm, Sweden. Report 5518.
- Börling, K., Otabbong, E., Barberis, E., 2001. Phosphorus sorption in relation to soil properties in some cultivated Swedish soils. *Nutr. Cycl. Agroecosyst.* 59, 39–46. <https://doi.org/10.1023/A:1009888707349>.
- Braghiere, R.K., Fisher, J.B., Allen, K., Brzostek, E., Shi, M., Yang, X., Ricciuto, M., Fisher, R.A., Phillips, R.P., 2022. Modeling global carbon costs of plant nitrogen and phosphorus acquisition. *J. Adv. Model. Earth. Sy.* 14, e2022MS003204 <https://doi.org/10.1029/2022MS003204>.
- Braun, S., Warrinnier, R., Börjesson, G., Ulén, B., Smolders, E., Gustafsson, J.P., 2019. Assessing the ability of soil tests to estimate labile phosphorus in agricultural soils: evidence from isotopic exchange. *Geoderma* 337, 350–358. <https://doi.org/10.1016/j.geoderma.2018.09.048>.
- Carlgrén, K., Mattsson, L., 2001. Swedish soil fertility experiments. *Acta Agric. Scand.* B51, 49–76. <https://doi.org/10.1080/090647101753483787>.
- Celi, L., Lamacchia, S., Marsan, F.A., Barberis, E., 1999. Interaction of inositol hexaphosphate on clays: adsorption and charging phenomena. *Soil Sci.* 164, 574–585. <https://doi.org/10.1097/00010694-199908000-00005>.
- De Bolle, S., De Neve, S., Hofman, G., 2013. Rapid redistribution of P to deeper soil layers in P-saturated acid sandy soils. *Soil Use Manage.* 29 (Suppl. 1), 76–82. <https://doi.org/10.1111/j.1475-2743.2012.00426.x>.
- Doherty, J., 2010. PEST. Model-independent parameter estimation. User manual, 5<sup>th</sup> Ed. Watermark Numerical Computing.
- Egnér, H., Riehm, H., Domingo, W., 1960. Untersuchungen über die chemische Bodenanalyse als Grundlage für die Beurteilung des Nährstoffzustandes der Böden. II. Chemische Extraktionsmethoden zur Phosphor- und Kaliumbestimmung. *Kungliga Lantbrukshögskolans Annaler* 26, 199–215.
- Eriksson, A.K., Hesterberg, D., Klysubun, W., Gustafsson, J.P., 2016. Phosphorus dynamics in Swedish agricultural soils as influenced by fertilization and mineralogical properties: insights gained from batch experiments and XANES spectroscopy. *Sci. Total Environ.* 566–567, 1410–1419. <https://doi.org/10.1016/j.scitotenv.2016.05.225>.
- Freese, D., van Riemsdijk, W.H., van der Zee, S.E.A.T.M., 1995. Modelling phosphate-sorption kinetics in acid soils. *Eur. J. Soil Sci.* 46, 239–245. <https://doi.org/10.1111/j.1365-2389.1995.tb01832.x>.
- Goldberg, S., Sposito, G., 1984. A chemical model of phosphate adsorption by soils: II. Noncalcareous soils. *Soil Sci. Soc. Am. J.* 48, 779–783. <https://doi.org/10.2136/sssaj1984.03615995004800040016x>.
- González Rodríguez, I., Yli-Halla, M., Jaakkola, A., 2018. Fate of phosphorus in soil during a long-term fertilization experiment in Finland. *J. Plant Nutr. Soil Sci.* 181, 675–685. <https://doi.org/10.1002/jpln.201800038>.
- Gustafsson, J.P., 2001. Modeling the acid-base properties and metal complexation of humic substances with the Stockholm Humic Model. *J. Coll. Interf. Sci.* 244, 102–112. <https://doi.org/10.1006/jcis.2001.7871>.
- Gustafsson, J.P., 2023. PBalD8 – a scenario tool for phosphorus mass balances in soils. Last accessed 2023-05-22 Web. <http://vminteq.com/pbalD8/>.
- Gustafsson, J.P., Mwamila, L.B., Kergoat, K., 2012. The pH dependence of phosphate sorption and desorption in Swedish agricultural soils. *Geoderma* 189–190, 304–311. <https://doi.org/10.1016/j.geoderma.2012.05.014>.
- Gustafsson, J.P., Braun, S., Tuyishime, J.R.M., Adedirán, G.A., Warrinnier, R., Hesterberg, D., 2020. A probabilistic approach to phosphorus speciation of soils using P K-edge XANES spectroscopy with linear combination fitting. *Soil Sys.* 4, 26. <https://doi.org/10.3390/soilsystems4020026>.
- Gustafsson, J.P., 2022. LCF-Linear. Web: <https://vminteq.com/lcf-linear/> (Last accessed 2023-05-22).

- Hiemstra, T., van Riemsdijk, W.H., 1996. A surface structural approach to ion adsorption: the charge distribution (CD) model. *J. Coll. Interf. Sci.* 179, 488–508. <https://doi.org/10.1006/jcis.1996.0242>.
- ISO, International Organization for Standardization, 2009. Soil quality — determination of particle size distribution in mineral soil material — method by sieving and sedimentation. ISO 11277, Geneva, Switzerland.
- Jaakkola, A., Hartikainen, H., Lemola, R., 1997. Effect of fertilization on soil phosphorus in a long-term field experiment in southern Finland. *Agric. Food Sci. Finland* 6, 313–322. <https://doi.org/10.23986/afsci.72794>.
- Johansson, L., Gustafsson, J.P., 2000. Phosphate removal using blast furnace slag and opoka — mechanisms. *Wat. Res.* 34, 259–265. [https://doi.org/10.1016/S0043-1354\(99\)00135-9](https://doi.org/10.1016/S0043-1354(99)00135-9).
- Jones, C.A., Cole, C.V., Sharpley, A.N., Williams, J.R., 1984. A simplified soil and plant phosphorus model: I Documentation. *Soil Sci. Soc. Am. J.* 48, 800–805. <https://doi.org/10.2136/sssaj1984.03615995004800040020x>.
- Jordan-Meille, L., Rubaek, G.H., Ehler, P.A.I., Genot, V., Hofman, G., Goulding, K., Recknagel, J., Provolò, G., Barraclough, P., 2012. An overview of fertilizer-P recommendations in Europe: soil testing, calibration and fertilizer recommendations. *Soil Use Manage.* 28, 419–435. <https://doi.org/10.1111/j.1475-2743.2012.00453.x>.
- Kirchmann, H., 1991. Properties and classification of soils of the Swedish long-term fertility experiments. I. Sites at Fors and Kungsängen. *Acta Agric. Scand.* 41, 227–242. <https://doi.org/10.1080/00015129109439905>.
- Kirchmann, H., Eriksson, J., Snäll, S., 1999. Properties and classification of soils of the Swedish long-term fertility experiments. IV. Sites at Ekebo and Fjärdingslöv. *Acta Agric. Scand. Sect. B. Soil and Plant Sci.* 49, 25–38. <https://doi.org/10.1080/09064719950135678>.
- Kirchmann, H., Snäll, S., Eriksson, J., Mattsson, L., 2005. Properties and classification of soils of the Swedish long-term fertility experiments: V. Sites at Vreta Kloster and Högåsa. *Acta Agric. Scand. Sect. B. Soil and Plant Sci.* 55, 98–110. <https://doi.org/10.1080/09064710510008711>.
- Klysubun, W., Tarawarakarn, P., Thamsanong, N., Amonpattaratkit, P., Cholsuk, C., Lapboonrueng, S., Chaichuay, S., Wongtepa, W., 2020. Upgrade of SLRI BL8 beamline for XAFS spectroscopy in a photon energy range of 1–13 keV. *Radiat. Phys. Chem.* 175, 108145. <https://doi.org/10.1016/j.radphyschem.2019.02.004>.
- Koopmans, G.F., Chardon, W.J., de Willigen, P., van Riemsdijk, W.H., 2004. Phosphorus desorption dynamics in soil and the link to a dynamic concept of bioavailability. *J. Environ. Qual.* 33, 1393–1402. <https://doi.org/10.2134/jeq2004.1393>.
- Lookman, R., Freese, D., Merckx, R., Vlassak, K., van Riemsdijk, W.H., 1995. Long-term kinetics of phosphate release from soil. *Environ. Sci. Technol.* 29, 1569–1575. <https://doi.org/10.1021/es00060a020>.
- McGechan, M.B., Lewis, D.R., 2002. Sorption of phosphorus by soil, part 1: principles, equations and models. *Biosys. Eng.* 82, 1–24. <https://doi.org/10.1006/bioe.2002.0054>.
- McGivney, E., Gustafsson, J.P., Belyazid, S., Zetterberg, T., Löfgren, S., 2019. Assessing the impact of acid rain and forest harvest intensity with the HD-MINTEQ model — soil chemistry of three Swedish conifer sites from 1880 to 2080. *Soil* 5, 63–77. <https://doi.org/10.5194/soil-5-63-2019>.
- Messiga, A.J., Ziadi, N., Bélanger, G., Morel, C., 2012. Process-based mass-balance modeling of soil phosphorus availability in a grassland fertilized with N and P. *Nutr. Cycl. Agroecosyst.* 92, 273–287.
- Messiga, A.J., Ziadi, N., Mollier, A., Parent, L.-E., Schneider, A., Morel, C., 2015. Process-based mass-balance modeling of soil phosphorus availability: testing different scenarios in a long-term maize monoculture. *Geoderma* 243–244, 41–49. <https://doi.org/10.1016/j.geoderma.2014.12.009>.
- Morel, C., Ziadi, N., Messiga, A., Bélanger, G., Denoroy, P., Jeangros, B., Jouany, C., Fardeau, J.-C., Mollier, A., Parent, L.-E., Proix, N., Rabeharisoa, L., Sinaj, S., 2014. Modeling of phosphorus dynamics in contrasting agroecosystems using long-term field experiments. *Can. J. Soil Sci.* 94, 377–387. <https://doi.org/10.4141/cjss2013-024>.
- Mundus, S., Carstensen, A., Husted, S., 2017. Predicting phosphorus availability to spring barley (*Hordeum vulgare*) in agricultural soils of Scandinavia. *Field Crops Res.* 212, 1–10. <https://doi.org/10.1016/j.fcr.2017.06.026>.
- Nye, P.H., Tinker, P.B., 1977. Solute movement in the soil-root system. *Studies in ecology* (Vol. 4). Blackwell Scientific Publications, Oxford, U.K.
- Ohno, T., Zibilske, L.M., 1991. Determination of low concentrations of phosphorus in soil extracts using malachite green. *Soil Sci. Soc. Am. J.* 55, 892–895. <https://doi.org/10.2136/sssaj1991.03615995005500030046x>.
- Olsen, S., Cole, C., Watanabe, F., Dean, L., 1954. Estimation of available phosphorus in soils by extraction with sodium bicarbonate. USDA Circular, 939. US Gov. Print. Office, Washington.
- Radcliffe, R.E., Reid, D.K., Blombäck, G., Bolster, C.H., Collick, A.S., Easton, Z.M., Francesconi, W., Fuka, D.R., Johnson, H., King, K., Larsbo, M., Youssef, M.A., Mulkey, A.S., Nelson, N.O., Persson, K., Ramirez-Avila, J.J., Schmieder, F., Smith, D., 2015. Applicability of models to predict phosphorus losses in drained fields: a review. *J. Environ. Qual.* 44, 614–628. <https://doi.org/10.2134/jeq2014.05.0220>.
- Ravel, B., Newville, M., 2005. Athena, artemis, hephaestus: data analysis for X-ray absorption spectroscopy using IFEFFIT. *J. Synchrotron. Radiat.* 12, 537–541. <https://doi.org/10.1107/S0909049505012719>.
- Römken, M.J.M., Nelson, D.W., 1974. Phosphorus relationships in runoff from fertilized soils. *J. Environ. Qual.* 3, 10–13. <https://doi.org/10.2134/jeq1974.00472425000300010003x>.
- Rubaek, G.H., Kristensen, K., Olesen, S.E., Østergaard, H.S., Heckrath, G., 2013. Phosphorus accumulation and spatial distribution in agricultural soils in Denmark. *Geoderma* 209–210, 241–250. <https://doi.org/10.1016/j.geoderma.2013.06.022>.
- Schackelford, C.D., Daniel, D.E., 1991. Diffusion in saturated soil. I: background. *J. Geotech. Eng. ASCE* 117, 467–484. [https://doi.org/10.1061/\(ASCE\)0733-9410\(1991\)117:3\(467\)](https://doi.org/10.1061/(ASCE)0733-9410(1991)117:3(467)).
- Seidel, S.J., Gaiser, T., Ahrends, H.E., Hüging, H., Siebert, S., Bauke, S.L., Gocke, M.I., Koch, M., Schweitzer, K., Schaaf, G., Ewert, F., 2021. Crop response to P fertilizer omission under a changing climate — experimental and modeling results over 115 years of a long-term fertilizer experiment. *Field Crop Res.* 268, 108174. <https://doi.org/10.1016/j.fcr.2021.108174>.
- Sharpley, A.N., Jones, C.A., Gray, C., Cole, C.V., 1984. A simplified soil and plant phosphorus model: II. Prediction of labile, organic and sorbed phosphorus. *Soil Sci. Soc. Am. J.* 48, 805–809.
- Sibbesen, E., Skjøth, F., Rubaek, G., 2000. Tillage caused dispersion of phosphorus and soil in four 16-year old field experiments. *Soil Tillage Res.* 54, 91–100. [https://doi.org/10.1016/S0167-1987\(00\)00888-X](https://doi.org/10.1016/S0167-1987(00)00888-X).
- Siebers, N., Wang, L., Funk, T., von Tucher, S., Merbach, I., Schweitzer, K., Kruse, J., 2021. Subsoils — a sink for excess fertilizer P but a minor contribution to P plant nutrition: evidence from long-term fertilization trials. *Environ. Sci. Eur.* 33, 60. <https://doi.org/10.1186/s12302-021-00496-w>.
- Smolders, E., Nawara, S., De Cooman, E., Merckx, R., Martens, S., Elsen, A., Odeurs, W., Vandendriessche, H., Santner, J., Amery, F., 2021. The phosphate desorption rate in soil limits phosphorus bioavailability to crops. *Eur. J. Soil Sci.* 72, 221–233. <https://doi.org/10.1111/ejss.12978>.
- Svanbäck, A., Ulén, B., Etana, A., Bergström, L., Kleinman, P.J.A., Mattsson, L., 2013. Influence of soil phosphorus and manure on phosphorus leaching in Swedish topsoils. *Nutr. Cycl. Agroecosyst.* 96, 133–147. <https://doi.org/10.1007/s10705-013-9582-9>.
- Sverdrup, H., Warfvinge, P., 1993. Calculating field weathering rates using a mechanistic geochemical model PROFILE. *Appl. Geochem.* 8, 273–283. [https://doi.org/10.1016/0883-2927\(93\)90042-F](https://doi.org/10.1016/0883-2927(93)90042-F).
- Tattari, S., Bärlund, I., Rekolainen, S., Posch, M., Siimes, K., Tuhkanen, H.-R., Yli-Halla, M., 2001. Modeling sediment yield and phosphorus transport in Finnish clayey soils. *Transactions ASAE* 44, 297–307.
- Tipping, E., 1994. WHAM — a chemical equilibrium model and computer code for waters, sediments, and soils incorporating a discrete-site electrostatic model of ion binding by humic substances. *Comput. Geosci.* 20, 973–1023. [https://doi.org/10.1016/0098-3004\(94\)90038-8](https://doi.org/10.1016/0098-3004(94)90038-8).
- Tuyishine, J.R.M., Adediran, G.A., Olsson, B.A., Spohn, M., Hillier, S., Klysubun, W., Gustafsson, J.P., 2022. Phosphorus abundance and speciation in acid forest Podzols — effect of postglacial weathering. *Geoderma* 406, 115500. <https://doi.org/10.1016/j.geoderma.2021.115500>.
- Van der Bom, F.J.T., McLaren, T.I., Doolette, A.L., Magid, J., Frossard, E., Oberson, A., Jensen, L.S., 2019. Influence of long-term phosphorus fertilisation history on the availability and chemical nature of soil phosphorus. *Geoderma* 355, 113909. <https://doi.org/10.1016/j.geoderma.2019.113909>.
- Van der Salm, C., Kros, J., de Vries, W., 2016. Evaluation of different approaches to describe the sorption and desorption of phosphorus in soils on experimental data. *Sci. Total Environ.* 571, 292–306. <https://doi.org/10.1016/j.scitotenv.2016.07.004>.
- Van der Zee, S.E.A.T.M., van Riemsdijk, W.H., 1988. Model for long-term phosphate reaction kinetics in soil. *J. Environ. Qual.* 17, 35–41. <https://doi.org/10.2134/jeq1988.00472425001700010005>.
- Van Rheeuwijk, L., 1995. Procedures for soil analysis. *Int. Soil Ref. Inf. Centre, Wageningen, Netherlands*.
- Walker, T., Adams, A., 1958. *Studies on soil organic matter: I. Influence of phosphorus content of parent materials on accumulations of carbon, nitrogen, sulphur, and organic phosphorus in grassland soils.* *Soil Sci.* 85, 307–318.
- Wolf, A.M., Baker, D.E., 1990. Colorimetric method for phosphorus measurement in ammonium oxalate soil extracts. *Commun. Soil Sci. Plant Anal.* 21, 2257–2263. <https://doi.org/10.1080/00103629009368378>.
- Zicker, T., von Tucher, S., Kavka, M., Eichler-Löbermann, B., 2018. Soil test phosphorus as affected by phosphorus budgets in two long-term field experiments in Germany. *Field Crops Res.* 218, 158–170. <https://doi.org/10.1016/j.fcr.2018.01.008>.